Accepted Manuscript

Title: Cholesteryl to improve the cellular uptake of Polymersomes within HeLa cells

Author: Chloe Martin Nino Marino Ciara Curran Anthony P. McHale John F. Callan Bridgeen Callan

PII: S0378-5173(16)30666-4
DOI: http://dx.doi.org/doi:10.1016/j.ijpharm.2016.07.036
Reference: IJP 15933

To appear in: *International Journal of Pharmaceutics*

Received date: 13-5-2016
Revised date: 15-7-2016
Accepted date: 16-7-2016

Please cite this article as: Martin, Chloe, Marino, Nino, Curran, Ciara, McHale, Anthony P., Callan, John F., Callan, Bridgeen, Cholesteryl to improve the cellular uptake of Polymersomes within HeLa cells.International Journal of Pharmaceutics http://dx.doi.org/10.1016/j.ijpharm.2016.07.036

Cholesteryl to improve the cellular uptake of Polymersomes within HeLa cells.

Chloe Martin[a], Nino Marino[a], Ciara Curran[a], Anthony P. McHale[a], John F. Callan[a] and Bridgeen Callan[a*].

[a]School of Pharmacy and Pharmaceutical Sciences, The University of Ulster, Northern Ireland, BT52 1SA.

*Corresponding author at: School of Pharmacy and Pharmaceutical Sciences, The University of Ulster, Northern Ireland, BT52 1SA. Tel: +28 70 123510 Fax: +28 70 123518 b.callan@ulster.ac.uk

GRAPHICAL ABSTRACT

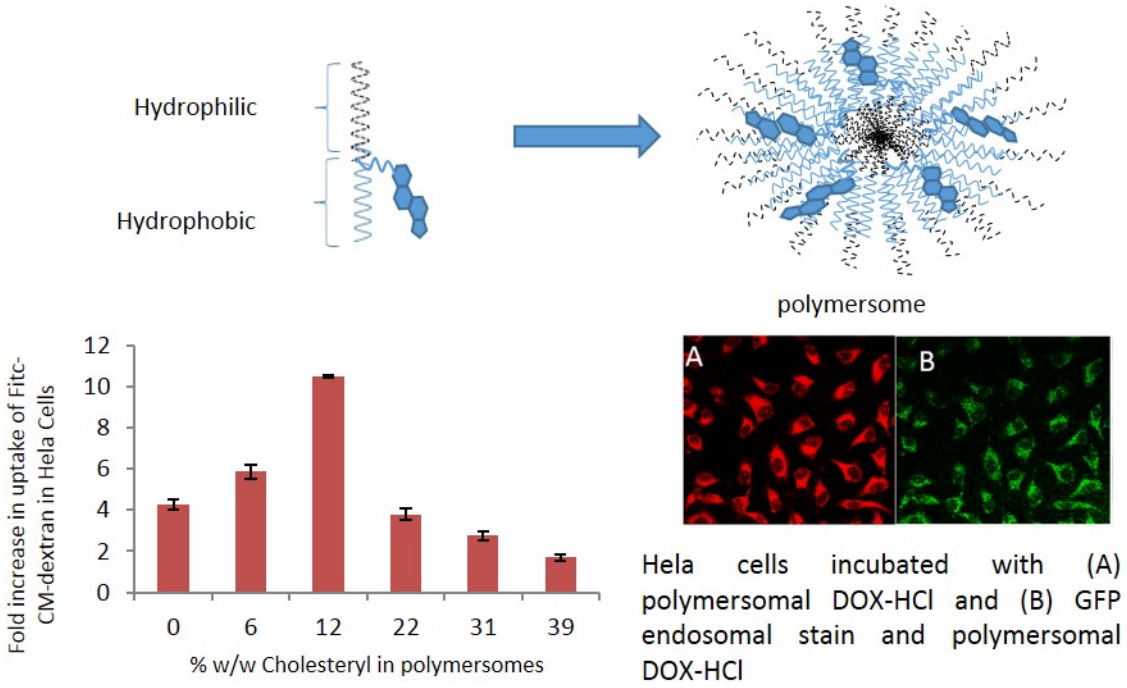

Abstract

The need to develop a greater understanding of drug delivery systems has arisen through the development of alternative biological based therapeutics. Drug delivery systems need to adapt and respond to this increasing demand for cellular transportation of highly charged species. Polymersomal drug delivery systems have displayed great potential and versatility for such a task. In this manuscript we present the synthesis, characterisation and biological evaluation of six amphiphilic random co polymers with varying amounts of cholesteryl (0-39 %wt) before the subsequent formation into polymersomes. The polymersomes were then analysed for size, zeta potential, encapsulation efficiency, release kinetics and cellular uptake. Results confirmed that the polymersome containing 12 %wt cholesteryl polymer displayed a ten-fold increase in cellular uptake of Fitc-CM-dextran when compared to un-encapsulated drug, crossing the cellular membrane via endocytosis. The size of these vehicles ranged between 100 – 500 nm, zeta potential was shown to be neutral at -0.82 mV ±0.2 with encapsulation efficiencies in the region of 60 %. The ease of

adaptability and preparation of such systems renders them a viable alternative to liposomal drug delivery systems.

Keywords

Drug Delivery System (DDS), Amphiphilic Polymer, Polymersome, Cholesteryl, poly(ethylene) glycol.

1. Introduction

Recent advances in therapeutics has seen an extensive exploration into personalised medicine; this has led to the focus shifting from the more common small molecule therapeutics to much larger, biological based compounds referred to as 'biologics'(Martin et al 2016) . These naturally occurring, large, complex molecules (mostly proteins, nucleotides and polypeptides), generally have a specific therapeutic target for example a certain genotype or protein receptor (Morrow and Felcone 2004). The introduction of such specificity leads to higher efficacy and fewer unwanted side effects when compared against general systemic delivery of non-selective therapeutics. However with these new favourable developments come new complications, particularly those surrounding the delivery of such high molecular weight and extensively hydrophilic molecules. Biologics, such as siRNA, possessing high solubility but low permeability are defined as Class III using the Bio pharmaceutics Classification System (BCS) (Dahan et al. 2009). Acknowledgement of the absence of an appropriate drug delivery system (DDS) to overcome these problems has led to extensive research into designing a suitable amphiphilic nano-scale vehicle to allow increased solubility, and facilitate permeation across the cell membrane to enable drugs such as biologics to exhibit their desired therapeutic effect at the target site (Bartfai et al. 2010; Khan et al. 2010, Lin et al. 2004).

Nano-carriers such as liposomes, micelles, nanocapsules and polymersomes, offer many advantages over free drug administration and greatly improve the solubility of encapsulated or adsorbed drug compounds. They also protect drugs against degradation once administered (Fomina et al. 2012), allow various routes of administration including oral or inhalation (Gandhi et al. 2014) and most

importantly improve drug targeting and efficacy. This can occur either actively- by incorporating targeting moieties such as RGD-containing peptides, folic acid and carbohydrates (Khan et al. 2010); or passively- through the enhanced permeability and retention effect (EPR) caused by a combination of leaky vasculature and insufficient lymphatic drainage (Pasparakis et al. 2014). This beneficially reduces off site toxicity which is a major limiting factor in chemotherapy, as well as minimising resistance and allowing the delivery of more than one drug at a time by co-encapsulation (Dahan et al. 2009). The widely explored liposomal drug delivery system (DDS) first documented in 1965 by Bangham (Bangham 1993), successfully allows the delivery of both water soluble and insoluble drugs. However, being prepared from phospholipids can lead these carriers to possess leaky membranes resulting in premature release of payload. More recently polymersomes, which structurally mimic liposomes but are derived from the self-assembly of amphiphilic polymers, have become an attractive alternative due to the high loading ability of hydrophilic, hydrophobic or amphiphilic compounds allowing them to be exceptional in delivering bioactive molecules and combined loading of multi-drugs for synergistic therapy (Pasparakis et al. 2014; Bangham 1993). Their easily adaptable polymeric design, allied to the wide range of available co-polymers, means a wide variety of polymersome structures can be prepared with relative ease. By carefully choosing co-polymer blocks with specific chemical characteristics as well as altering the hydrophilic to hydrophobic ratio, a range of properties can be specifically tuned including size (Martin et al. 2015), encapsulation efficiency, pharmacokinetics including release rates (Alibolandi et al. 2015) , degradability and cellular uptake as well as highly stable membranes avoiding drug leakage (Xu et al. 2014). The use of Poly(ethylene) glycol (PEG) is well known in nanoparticle preparations for its steric shielding effect, leading to prolonged blood circulation time; its ability to reduce aggregation in serum; and its immuno-protection capabilities preventing elimination from the reticuloendothelial system (RES)(Xu et al. 2011; Kolli et al. 2013; Lee et al. 2001; Lee and Feijen 2012; Magarkar et al. 2012; Miyata et al. 2011; Wu and McMillan 2009). However, PEGylation has been reported to reduce cellular transfection and uptake by interference with intracellular trafficking but the dual

incorporation of PEG and lipid molecules such as cholesterol into nanoparticles is thought to provide a balance between prolonged circulation and essential targeted uptake (Xu et al. 2011). The importance of cholesterol in nanoparticle formulation is cemented by the FDA, which have only approved PEGylated liposomal drug delivery systems which incorporate cholesterol as a key component (Magarkar et al. 2012). Residing in the biological membranes of various organisms, it can modulate the fluidity of biological membranes involved in many important life events (Zhi-Yao et al. 2014). The role cholesterol plays in drug delivery systems is thought to involve packing and stability, directly affecting drug release rates and by enhancing cellular uptake: as it is recognised as a natural cell membrane component it is hypothesised that its inclusion will aid cellular uptake and transport across the cell membrane (Magarkar et al. 2012). Both liposomes and micelles formulated with cholesterol have shown increased cellular internalization, enhanced colloidal stability, higher encapsulation volumes and slower release of payload compared to without cholesterol (Magarkar et al. 2012; Zhi-Yao et al. 2014). Polymersomes have also been developed with cholesterol for enhanced purposes. Huang et al. (2013) developed a cholesterol containing polymersome (11.2 %wt) which was both amphoteric and amphiphilic. The increased electrostatic interactions within this polymer allow for a facile one step polymersome preparation, whereas the incorporation of cholesterol is credited with inhibiting binding to proteins and opsonins and enhancing cell uptake. Yin et al. (2014) dispersed cholesterol within the bilayer of a miktoarm star copolymer based polymersome and recorded both enhanced stability and cellular uptake of the resulting polymersome with a 1 %wt loading of cholesterol. Alternatively Jia et al. (2014) created a triggered release polymersome using an 80 %wt cholesterol containing polymer.

The need for enhanced drug delivery systems with high biocompatibility and cell permeability is of great interest to this area of pharmaceutics. The amount of cholesterol included within these drug delivery systems varies significantly between studies. In this work we present an enhanced polymersomal drug delivery system with cholesteryl incorporated within the architecture (Figure 1) of the polymer. By varying the amount of cholesteryl incorporated within six amphiphilic co-

polymers it was possible to identify the optimum concentration of cholesteryl to ensure the greatest cellular uptake while retaining the required encapsulation efficiency, release kinetics and hydrodynamic diameter. The comparative study presented in this work allows a better understanding of the influence of cholesteryl on cellular uptake.

2. Materials and Methods

Materials and Reagents

Chemicals were purchased from commercial sources at the highest possible purity and used as received. Poly(ethylene glycol) methacrylate (Mn 500 Da), fluorescein isothiocyanate-carboxymethyl-dextran (Fitc-CM-Dextran) (Mn 4KDa), methacrylic acid (99%) and 1-decanol (99%), ethylene diamine (99%), cholesteryl chloroformate (95%) and Thiazol Blue Tetrazolium Bromide (MTT)(98%) CellLight® Reagent BacMam 2.0 GFP were purchased form Sigma-Aldrich. DOX-HCl was purchased from VWR international.

2.1 Synthesis of Monomers

*2.1.1 Synthesis of Cholesteryl Ethylene-Diamine Conjugate (**3**)*

Compound **3** (10,13-dimethyl-17-(6-methylheptan-2-yl)-2,3,4,7,8,9,10,11,12,13,14,15,16,17-tetradecahydro-1H-cyclopenta[a]phenanthren-3-yl(2-aminoethyl)carbamate) was prepared by a method similar to that used by Sengupta et al. (2012). Briefly, ethylene diamine (6.26 ml, 93.7 mmol) (**2**) was dissolved in 20 ml of anhydrous dichloromethane (DCM) and cooled to 0 °C. Cholesteryl chloroformate (**1**) (3.0 g, 6.68mmol) in 20 ml of anhydrous DCM was added to the mixture and the reaction vigorously stirred for 18h. The contents were then washed with water (50 ml x 3) and brine (50 ml x 2). The final DCM layer was dried over anhydrous magnesium sulfate and the solvent removed under reduced pressure to afford the product as a white powder (2.7g, 85%).

*2.1.2 Synthesis of Intermediate compound 2,5-dioxopyrrolidin-1-yl methacrylate (**6**)*

To a 25 mL round-bottom flask were added 100 mg of methacrylic acid (**4**) (1.16 mmol), 160 mg of N-hydroxysuccinimide (**5**) (1.39 mmol), and 598 mg of dicyclohexylcarbodiimide (2.9 mmol). After 8 mL of dry acetonitrile was injected, the mixture was stirred under nitrogen for about 16-24 h at 25 °C. The whole process was monitored by TLC. After reaction, the suspension was filtered and the solution was evaporated by rotavapor under highly reduced pressure. The residue was purified by silica column chromatography (Exane/EtOAc, gradient from 4:1 to 3:2). The obtained compound was recrystallized from EtOAc and produced 200 mg of white powder (**6**). Yield: 86 %.

*2.1.3. Synthesis of Cholesteryl monomer (**7**)*

(10,13-dimethyl-17-(6-methylheptan-2-yl)-2,3,4,7,8,9,10,11,12,13,14,15,16,17-tetradecahydro-1H-cyclopenta[a]phenanthren-3-yl(2methacrylamidoethyl)carbamate) (**7**). A solution of **6** (100 mg, 0.54 mmol) in dry dichloromethane/DMF (1/1, 15 mL) under nitrogen was treated with **3** (258 mg, 0.54 mmol). The reaction mixture was stirred for 1 h at room temperature and the solvent removed under reduced pressure. Ethyl ether (60 mL) was added to the residue, washed with water (3 x 10 mL), brine (2 x 10 mL), dried over sodium sulphate and concentrated to dryness. Purification by silica gel chromatography eluting with 1:1 Exane/EtOAc gave **7** as a white solid (243 mg, 82%).

*2.1.4 Synthesis of Decyl Methacrylate Monomer (**9**)*

Monomer **9** was synthesised following a previously published method (Yildiz et al. 2011). 250 mg of methacrylic acid **4** (2.9 mmol), were added to 5 ml of 1-decanol **8** and sulfuric acid in catalytic amounts. The solution was stirred for 48 h at room temperature. After reaction the mixture was purified by silica gel chromatography eluting with Exane/EtOAc, gradient from 100% Exane to 95:5 to give compound **9** in quantitative yield.

2.2 Synthesis of Amphiphilic Polymers (**11 – 16**)

Methacrylate monomers, comprising different molar ratios of **7** and **9,** were added to a Carius reaction vessel together with poly (ethylene) glycol methacrylate (**10**) in anhydrous tetrahydrofuran according to the molar ratios described in Table 2. Approximately 0.3 molar ratio of free radical

generator 1,1'Azobis (cyclohexanecarbonitrile) (AICN): polymer was also added to the vessel. After three consecutive freeze-pump-thaw cycles the reaction vessel was sealed under vacuum at 80 °C for72 hours. THF (20mls) and hexane (20mls) were added and the contents centrifuged at 6000rpm for 5 min, the supernatant was discarded and the resulting pellet re-dissolved in THF and hexane. This was repeated 3 times.

The resulting pellet was dried under vacuum to leave the resultant amphiphilic co-polymers (**11** - **16**) as an oil.

2.3 Product Characterisation

2.3.1 Characterisation by Nuclear Magnetic Resonance (NMR)

^{1}H Nuclear Magnetic Resonance was carried out on all products synthesised. Samples were prepared using 10mgs of sample dissolved in 1 ml of deuterated chloroform and analysed using a Varian 500MHz Instrument.

2.3.2 Characterisation of monomers by Mass Spectrometry (MS)

1mg of sample was added to a glass vial with equal amounts of DCM and methanol. The sample was diluted with absolute methanol prior to measurement. The measurement occurred in positive electrospray mode via direct infusion.

2.4 Preparation of Polymersomes

Six polymersomes were prepared using the polymer ratios described in Table 2. They were prepared by creating a thin film (1mg) of a particular co-polymer (**11 – 16**) in chloroform ($CHCl_3$) (phase 1) then adding 100 µL 2.5mg/ml Fitc-CM-Dextran in phosphate buffered saline (PBS). The mixture was evaporated to dryness, purged with compressed air for 30 sec., before being suspended in 1.5-2ml dry chloroform. A further 1mL 2.5mg/ml of the identical polymer used in phase 1 but in PBS (phase 2) was added and the solution sonicated using a Branson 3510 bath sonicator (230V) at room

temperature for 2-5 minutes. The organic solvent was removed from the emulsion under reduced pressure at 40 ^{o}C.

2.5 Evaluation of Polymersomes

2.5.1 Hydrodynamic radius determined by Dynamic Light Scattering (DLS)

The polymersome solutions were suitably diluted to analyse the particle size distribution and zeta potential (+/- mV) using dynamic light scattering (DLS). The samples were diluted using sterile PBS and all measurements taken at room temperature on a Malvern Nano-ZS zetasizer using a glass/quartz cuvette. The hydrodynamic radius and zeta potential are quoted as size/charge ± standard error of the mean.

2.5.2. Scanning electron Microscopy (SEM)

Blank polymersomes were prepared from polymer **13** and added onto aluminium metal stubs in aqueous solution. Samples were then left covered to air dry before being sputter coated with gold and palladium. The images were recorded using a FEI Quanta SEM under a high vacuum in secondary electron mode.

2.5.3. Determination of Encapsulation Efficiency (%EE)

Encapsulation Efficiency was carried out by preparing polymersomes using the method above and encapsulating FITC-CM- Dextran. Polymersome solutions were diluted to 5ml with PBS and the sample placed in pre-purged Amicon filters (MWCO 30kDa) and centrifuged at 10000 x g for 30minutes at 4ºC. The samples were analysed using a Varian Cary Eclipse fluorescence spectrometer using 1 cm quartz cells with an excitation wavelength of 490 nm, slit width of 5 nm and collecting the emission between 520 and 620 nm. A standard calibration graph was prepared with the equation of the line:

$y = 21366x$ *where y = spectral area between 510 and 700 nm and x = concentration of fitc-CM-dextran (µM)*

The % encapsulation efficiency was determined from the following equation:

$\frac{FD_{Intensity}}{FO_{intensity}} \times 100\ \%$ *where FD = fluorescence intensity of Fitc-CM-Dextran following centrifugation and F0= fluorescence intensity of Fitc-CM-Dextran added*

2.5.4. Release of FITC CM Dextran from Polymersomes

Polymersomes loaded with FITC-CM-Dextran (1.25 mg) were prepared from polymer **13** using the method described previously in section 2.4. Any un-encapsulated fluorophore was removed by centrifugation at 10000 x g using a pre-purged Amicon filter (MWCO 30 kDa) for 30 min at 4 °C. Aqueous polymersomes of known FITC concentration (determined by fluorescence) were made up to a volume of 0.5ml using PBS and placed in dialysis tubing (MWCO 12kDa) in 20mls of PBS at 37 °C stirring and covered in foil. Measurements of fluorescence were taken at intervals over a 24 h period under sink conditions and analysed in the method described above using the Cary Eclipse fluorescence spectrophotometer.

2.6. In-Vitro Evaluation of Polymersomes

2.6.1 Uptake of encapsulated Fitc-CM-dextran into HeLa cells

Hela cells were cultured in Hams F-12 nutrient mixture and supplemented with Foetal Bovine Serum (10 %), penicillin (200 U mL^1), streptomycin (200 µg mL^1) and glutamine (2 mM). After reaching confluence, the cells were harvested by trypsinization and seeded in a 96 well plate at a density of 5000 cells per well and left overnight at 37 °C with 5 % CO_2, 20 % O_2. Cells were then washed twice with 100 µl PBS and 160 µl of fresh media added. Cells were spiked with relative controls (PBS and free Fitc-CM- Dextran) and polymersome solutions containing 0.1 mg/mL Fitc-CM-dextran in 0.7 mg/ml polymersome and incubated for a further 5 h at the conditions stated above. The aqueous content was then removed and each well washed twice with 200 µl of PBS and replaced with a

further 200 µl of PBS before fluorescence was recorded using a BMG Labtech Omega micro plate reader (excitation wavelength 485 nm and emission collected at 520 nm). Fluorescence values then used to work out concentration of FITC taken up by cells by using standard calibration curves established for free FITC Dextran and FITC encapsulated inside each polymersome.

2.6.2. *Confocal Imaging to determine uptake mechanism*

Hela cells were cultured in Hams F-12 nutrient mixture and supplemented with Foetal Bovine Serum (10 %), penicillin (200 U mL^{1}), streptomycin (200 µg mL^{1}) and glutamine (2 mM). After reaching confluence, the cells were harvested by trypsinization and seeded at a density of 2×10^4 cells mL^{-1} in a 96-well plate. The cells were incubated at 37 °C with O_2/CO_2/air (20:5:75, v/v/v) overnight and then in the presence of either free DOX-HCl or polymersomal DOX-HCl (14.4 ug/ml) for 5 h, following which time the media was removed and each well washed twice with 200 µl PBS (pH = 7.2) with 180 µl media replaced along with 20 µl CellLight® Reagent BacMam 2.0 GFP and the well plate incubated overnight in the conditions described above. The images were recorded on an inverted Leica SP5 confocal microscope, using an excitation wavelength of 470 nm and collecting the emission between 494 and 560 nm.

3. Results and Discussion

*3.1 Characterisation of monomer **7***

Monomer **7** was synthesised according to the procedure shown in Scheme 1. Cholesteryl chloroformate was first reacted in a 1:14 stoichiometry with ethylene diamine in an overnight reaction to yield the corresponding amide (**3**). The structure of this intermediate compound was confirmed by MS ([M+H] = 474.3 m/z) and ^{1}H NMR (data displayed in Figure 2). The additional peaks at 2.8 and 3.2 ppm, not present in the precursor compound **1** were attributed to the methylene protons associated with the new ethyl chain bridging the amide and amine functionalities. In addition, the proton on position C-2 of the steroidal cyclopentanoperhydrophenanthrene ring was

shifted upfield from 4.7ppm to 4.5 ppm indicative of the increased shielding provided by the amine that replaced the acid chloride. Compound **3** was then reacted with compound **6** in dry organic solvent at room temp for 1h. The successful synthesis of **7** was again confirmed using MS and ^{1}H NMR spectroscopy. The base peak at 564 Da was consistent with the sodium adduct of the molecular ion i.e. M^{+} + 23 (Na^{+} ion). The ^{1}H NMR spectrum is shown in Figure 2. These data confirm product formation with the olefinic protons of the methacrylate moiety clearly observed as diastereotropic peaks at 5.36 and 5.76 ppm with the additional methyl protons from the methacrylic unit as a singlet at 3.19ppm. The detailed NMR characterisation of compound **7** can be seen in Figure 3 with the corresponding peak allocation in Table 1.

*3.2. Characterisation of Polymers **11 – 16***

The polymers were synthesised according to scheme 2 with the specific molar ratios employed given in Table 2. The polymers were characterised using ^{1}H NMR as shown in Figure 4. Figure 4 shows the stacked spectra of the three individual monomers (**7**, **9** and **10**) in addition to polymer **13** and clearly indicates successful polymer formation. All the olefinic resonances present at ~5.4 and ~6.0 ppm in each of the monomers are absent in the polymer spectrum indicating the formation of a new carbon-carbon sigma bond. In addition, the spectrum of the polymer contains peaks corresponding to each of the monomers. Moreover, the resonances in the up-field region are much broader in the polymer spectrum than for the corresponding monomers. Such peak broadening is common for protons in or near the backbone of polymers and is due to an averaging of the chemical shift anisotropies. The spectrum of **13** is also dominated by the large characteristic PEG protons at ~3.5 ppm due to the high molar incorporation of this monomer within the polymer chain.

3.3 Characterisation of Polymersomes

3.3.1 Dynamic Light Scattering (DLS)

The polymersome formulations all had a hydrodynamic radius of < 600 nm rendering them suitable for cellular uptake via endocytosis. There was a general increase in size with increasing cholesteryl content, through linearity was poor with an R^2 of 0.78. A significant increase in hydrodynamic radius was observed for polymersome **16** (Table 3). This particular polymersome contained no carbon-10 chains, only PEG and cholesteryl, thus implying that the alkyl chain plays a significant role in the interdigitation of the polymersome bilayer. We have previously shown polymersomes to be size tuneable using this method of preparation however, for this study all parameters were kept consistent so as to allow a direct comparison between the hydrodynamic radius of polymersomes. Contrary to our results, the incorporation of cholesterol into polymer domains has been documented to cause reduced membrane thickness of synthesised nanoparticles (Huang et al. 2013; Magarkar et al. 2012; Yin et al. 2014). However, when incorporated into polymersomes it would appear to have the opposite effect, perhaps due to the small size of the polymersomes to begin with. Size is hugely important in ensuring polymersomes can reach and be internalised into target cells, if too small they will be unable to encapsulate significant amounts of active agent and if too large they may be quickly cleared by renal excretion and have issues crossing the cell membrane (Tanner et al. 2011; Jaskiewicz et al. 2012). It has been considered that polymersomes with a diameter of around 100nm are the most suitable for drug carrier systems due to their ability to evade detection by RES and an appropriate size for retention in tumour vasculature by the EPR effect (Jia et al. 2014). All polymers produced polymersomes of desired nano-size with good polydispersity.

Polydispersity Index (PDI) was measured for each of the polymersome samples. Results ranged between 0.37 - 0.76, this indicates a relatively good degree of polydispersity. However, some degree of aggregation of particles is implied and again in particular for polymer **16**, this could suggest that rather than a large increase in polymersome hydrodynamic radius, instead we are seeing an increase in aggregation between polymersomes or the creation of cholesteryl domains.

3.3.2. Encapsulation Efficiencies (% EE)

In order to establish the encapsulating ability of polymersomes prepared from polymers **11** -**16**, the fluorescent probe Fitc-CM-Dextran (4 kDa) was used as a hydrophilic model dye which accumulates in the aqueous core of the system at a loading capacity of 12.5 % wt:wt (wt of fluorophore: total DDS wt). As can be seen from Table 3, the encapsulation efficiencies of all the polymersomes tested did not vary significantly, this is as expected due to the hydrophilic component of these DDS remaining unchanged. The PEG is responsible for the creation of the inner hydrophilic core of this system, and it is anticipated that any hydrophilic component will reside within this hydrophilic environment. The results detailed in table 3 ranged between 52 – 60 % encapsulation efficiency. These results are in keeping with a previous study where we determined the encapsulation efficiency of polymersomes prepared from polymer **11** to have a % EE of 53 % at 12.5 % wt: wt loading. We have also shown that this % EE can be increased to > 70 % if the amount of drug loading is significantly reduced (Martin et al. 2015).

3.3.3. FITC Dextran Release from Polymersomes

Release of hydrophilic fluorescent Fitc-CM-dextran from polymersomes was established under sink conditions at 37 °C. A maximum release rate was observed within the first hour but this burst release then gave rise to a more constant rate observed from 2 - 24 hours. The percentage release value at 24 hours was 56 % (± 13.5) (Figure 5).

3.3.4 Scanning Electron Microscope (SEM) Imaging

Blank polymersomes (i.e. no drug encapsulated) prepared from polymer **13** were analysed by SEM. (Figure 6). The images reveal several clusters of sizes in the region of 100 nm to 200 nm with all of the polymersomes having the expected spherical morphology. The sizes of polymersomes observed were in the expected range and correspond with the results from DLS which show the same polymersome to have a hydrodynamic radius of 197 nm.

3.4. In-Vitro Evaluation of Polymersomes

3.4.1. Cellular Uptake of Polymersomes with Varying amounts of Cholesterol

Cellular uptake was established in Hela cells by encapsulating Fitc-CM-Dextran (MW = 4KDa) into the hydrophilic core of the polymersomes. Fitc-CM-Dextran was chosen as it is known to have poor cellular uptake due to its high water solubility and negative charge. All polymersomes were prepared as described with the dye incorporated within the core. Following incubation the media was removed and the cells washed with PBS before being analysed for intracellular Fitc-CM-Dextran content. The results of this study are shown in Figure 7 and have been compared to free FITC-CM-Dextran. Polymersomes formulated with the 12% w/w polymer (polymer **13**) showed the highest uptake of Fitc-CM-Dextran by HeLa cells. This was more than double the uptake observed with any of the other polymersomes containing cholesteryl and a ten-fold increase on the cellular uptake of un-encapsulated Fitc-CM-Dextran. All of the polymersomal systems prepared displayed an enhanced uptake when compared with the intracellular concentration of free Fitc-CM-Dextran within the HeLa cells (0.297 μg/ml). The lowest cellular uptake was observed for the polymersome containing no decyl units (prepared from polymer **16**), which may be due to the rigidity of the polymersome and greater hydrodynamic radius than any of the other prepared DDSs or the potential formation of aggregates preventing endocytosis. Indeed, this only serves to highlight the significance of tailoring and fine tuning the polymers prior to formulation into the DDS.

3.4.2. Confocal Imaging to determine uptake mechanism

In order to confirm the mechanism of cellular uptake, the late stage endosomal green fluorescent protein stain (CellLight® Reagent BacMam 2.0 GFP) was incubated in Hela cells alongside a polymersome formulated from polymer **13** that contained DOX-HCl. DOX-HCl was chosen as its absorbance and emission spectra enable simultaneous detection of both the encapsulated drug as well as the GFP endosomal stain. When comparing the bright field images of the cells with no DOX-HCl (A) to that of the free DOX-HCl (D) and polymersomal DOX-HCl (G), there is a clear difference in

the number of living cells (Figure 8). This is not unsurprising given the toxicity of DOX-HCl to the HeLa cell line. When we consider the DOX-HCl emission (560 – 620nm) from images B, E and H there appears to be a difference in the morphology of the cells that were exposed to free DOX-HCl (E) when compared to the polymersomal DOX-HCl (H). The cells exposed to free DOX-HCl have only minimal evidence of any late stage endosomes, whereas those exposed to the polymersomal DOX-HCl display a significant amount of late stage endosomes in all cells. This confirms that the mechanism of transport between the two forms of DOX-HCl is very different, with the polymersomal system transcending the cellular membrane via endocytosis whereas the free DOX-HCl does not. The mechanism of transport for the free DOX-HCl is most likely to be passive diffusion given the relatively low molecular weight of the drug.

4. Conclusion

In conclusion, the present study successfully demonstrates how cholesterol can be incorporated within polymersomal drug delivery systems to significantly increase cellular uptake. By the preparation and analysis of polymersomes containing between 0 and 39 % wt/wt cholesteryl we can conclude that a 12% wt /wt incorporation leads to a ten-fold increase in cellular uptake of encapsulated drug within Hela cells. In addition to the improved cellular uptake we have shown that the mechanism of transport of these systems is via endocytosis. The size of the DDSs increases with increasing cholesteryl content, and the presence of flexible ligands within the random co-polymer, such as the decyl chain, is required to enable the size of the polymersome to remain > 300nm. This data suggests that polymersomes are yet to reach their full capabilities in drug delivery systems and there is still much work required to reach their full potential.

Acknowledgements

The authors would like to thank the University of Ulster, the Department for Employment and Learning (DEL) Northern Ireland and the Dowager Countess Eleanor Peel Trust (grant number JWP 15/05-81) for their financial support.

5. References

Alibolandi, M. Sadeghi, F. Sazmand, S.H. Shahrokhi, S.M. Seifi, M. Hadizadeh, F. Synthesis and self-assembly of biodegradable polyethylene glycol-poly (lactic acid) diblock copolymers as polymersomes for preparation of sustained release system of doxorubicin, Int. J. Pharm. Investig. 5 (2015) 134–41.

Bangham, A. Liposomes - the Babaham connection, Chem. Phys. Lipids. 64 (1993) 275–285.

Bartfai, T. Lees, G. V. Drug Discovery: From Bedside to Wall Street, Academic Press, 2010.

Dahan, A. Miller, J.M. Amidon G.L., Prediction of solubility and permeability class membership: provisional BCS classification of the world's top oral drugs, AAPS J. 11 (2009) 740–6.

Fomina, N. Sankaranarayanan, J. Almutairi, A. Photochemical mechanisms of light-triggered release from nanocarriers, Adv. Drug Deliv. Rev. 64 (2012) 1005–20.

Gandhi, N.S. Tekade, R.K. Chougule, M.B. Nanocarrier mediated delivery of siRNA/miRNA in combination with chemotherapeutic agents for cancer therapy: current progress and advances, J. Control. Release. 194 (2014) 238–56.

Huang, Z. Teng, W. Liu, L. Wang, L. Wang, Q. Dong. Y.Efficient cytosolic delivery mediated by polymersomes facilely prepared from a degradable, amphiphilic, and amphoteric copolyer. Nanotech. 24 (2013) 265104.

Jaskiewicz, K. Larsen, A. chaeffel, D. S Koynov, K. Lieberwirth, I. Fytas, G. Landfester, K. Kroeger, A. Incorporation of nanoparticles into polymersomes: size and concentration effects, ACS Nano. 6 (2012) 7254–62.

Jia, L. Cui, D. Bignon, J. Di Cicco, A. Wdzieczak-Bakala, J. Liu, J. Li MH. Reduction-responsive cholesterol-based block copolymer vesicles for drug delivery, Biomacromolecules. 15 (2014) 2206–17.

Khan, F. Katara, R. Ramteke, S. Enhancement of bioavailability of cefpodoxime proxetil using different polymeric microparticles, AAPS PharmSciTech. 11 (2010) 1368–75.

Kolli, S. Wong, S.-P. Harbottle, R. Johnston, B. Thanou, M. Miller A.D. pH-triggered nanoparticle mediated delivery of siRNA to liver cells in vitro and in vivo, Bioconjug. Chem. 24 (2013) 314–32.

Lee, J.C. Bermudez, H. Discher, B.M. Sheehan, M.A. Won, Y.Y. Bates, F.S. Discher, D.E. Preparation, stability, and in vitro performance of vesicles made with diblock copolymers, Biotechnol. Bioeng. 73 (2001) 135–45.

Lee, J.S. Feijen, J. Polymersomes for drug delivery: design, formation and characterization., J. Control. Release. 161 (2012) 473–83.

Lin, J.J. Silas, J.A. Bermudez, H. Milam, V.T. Bates, F.S. Hammer, D.A. The effect of polymer chain length and surface density on the adhesiveness of functionalized polymersomes, Langmuir. 20 (2004) 5493–500.

Magarkar, A. Karakas, E. Stepniewski, M. Róg, T. Bunker, A. Molecular dynamics simulation of PEGylated bilayer interacting with salt ions: a model of the liposome surface in the bloodstream, J. Phys. Chem. B. 116 (2012) 4212–9.

Martin, C. Aibani, N. Callan, J.F. Callan, B. Recent advances in amphiphilic polymers for simultaneous delivery of hydrophobic and hydrophilic drugs, Ther. Deliv. 7 (2016) 15–31.

Martin, C. Dolmazon, E. Moylan, K. Fowley, C. McHale, A.P. Callan, J.F. Callan, B. A charge neutral, size tuneable polymersome capable of high biological encapsulation efficiency and cell permeation, Int. J. Pharm. 481 (2015) 1–8.

Miyata, K. Christie, R.J. Kataoka, K. Polymeric micelles for nano-scale drug delivery, React. Funct. Polym. 71 (2011) 227–234.

Morrow, T. Felcone, L.H. Defining the difference: What Makes Biologics Unique, Biotechnol. Healthc. 1 (2004) 24–9.

Pasparakis, G. Manouras, T. Vamvakaki, M. Argitis, P. Harnessing photochemical internalization with dual degradable nanoparticles for combinatorial photo-chemotherapy, Nat. Commun. 5 (2014) 3623.

Sengupta, P. Basu, S. Soni, S. Pandey, A. Roy, B. Oh, M.S. Chin, K.T. Paraskar, A.S. Sarangi, S. Connor, Y. Sabbisetti, V.S. Kopparam, J. Kulkami, A. Muto, K. Amarasiriwardena, C. Jayawardene, I. Lupoli, N. Dinulescu, D.M. Bonventre, J.V. Mashelkar, R.A. Sengupta, S.Cholesterol-tethered platinum II-based supramolecular nanoparticle increases antitumor efficacy and reduces nephrotoxicity, Proc. Natl. Acad. Sci. 109 (2012) 11294–11299.

Tanner, P. Baumann, P. Enea, R. Onaca, O. Palivan, C. Meier, W.Polymeric vesicles: from drug carriers to nanoreactors and artificial organelles, Acc. Chem. Res. 44 (2011) 1039–49.

Wu, S.Y. McMillan, N.A.J. Lipidic systems for in vivo siRNA delivery, AAPS J. 11 (2009) 639–52.

Xu, L. Wempe, M.F. Anchordoquy, T.J. The effect of cholesterol domains on PEGylated liposomal gene delivery in vitro, Ther. Deliv. 2 (2011) 451–60.

Yildiz, I. Impellizzeri, S. Deniz, E. McCaughan, B. Callan, J.F. Raymo, F.M.Supramolecular strategies to construct biocompatible and photoswitchable fluorescent assemblies, J. Am. Chem. Soc. 133 (2011) 871–9. doi:10.1021/ja107341f.

Yin, H. Kang, H.C. Huh, K.M. Bae, Y.H. Effects of cholesterol incorporation on the physicochemical, colloidal, and biological characteristics of pH-sensitive AB_2 miktoarm polymer-based polymersomes, Colloids Surf. B. Biointerfaces. 116 (2014) 2128–37.

Zhi-Yao, H. Bing-Yang, C. Via-Wei, W. Jiao, L. Edwards, C.K. Xiang-Rong, S. Gu, H. Yong-Mei, X. Zhi-Yong, Q. Recent development of poly(ethylene glycol)-cholesterol conjugates as drug delivery systems, Int. J. Pharam. 469 (2014) 168- 178.

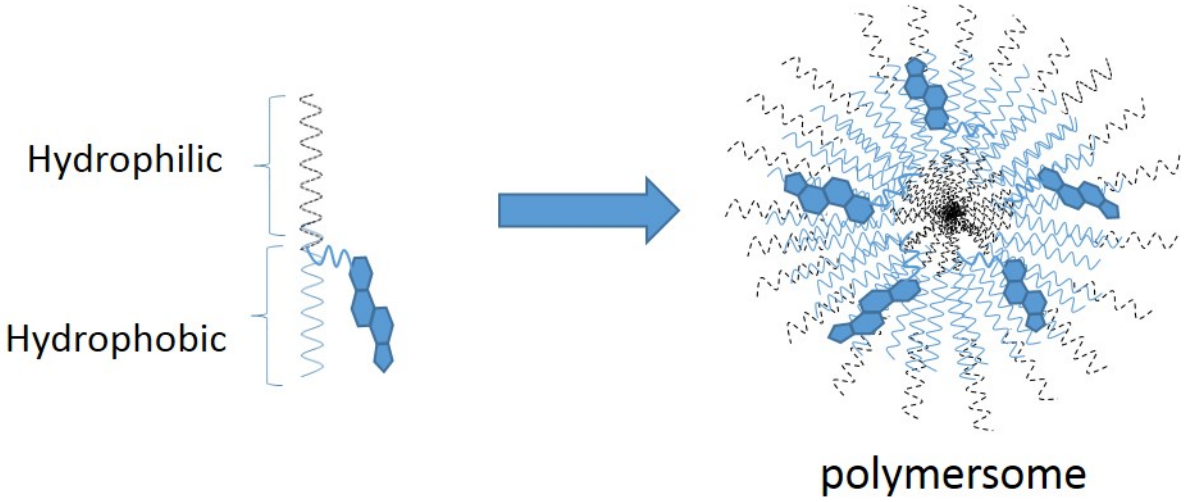

Figure 1. Polymersome formation with incorporated cholesteryl

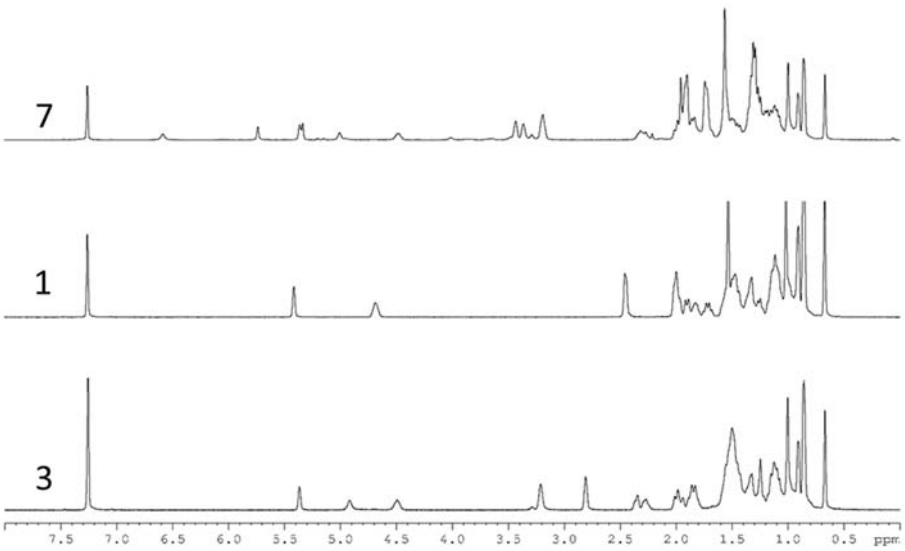

*Figure 2. Stacked 1H NMR (in $CDCl_3$) of starting material (**1**), intermediate (**3**) and monomer **5**.*

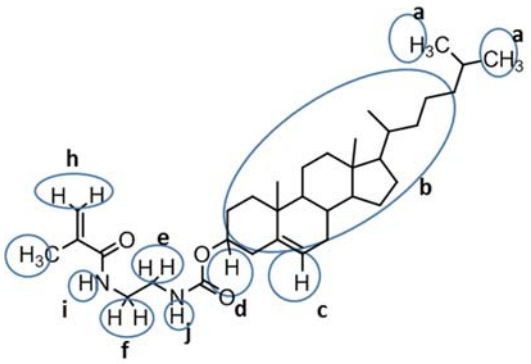

*Figure 3. Monomer **7** with specific protons identified for NMR analysis listed alphabetically from a – j.*

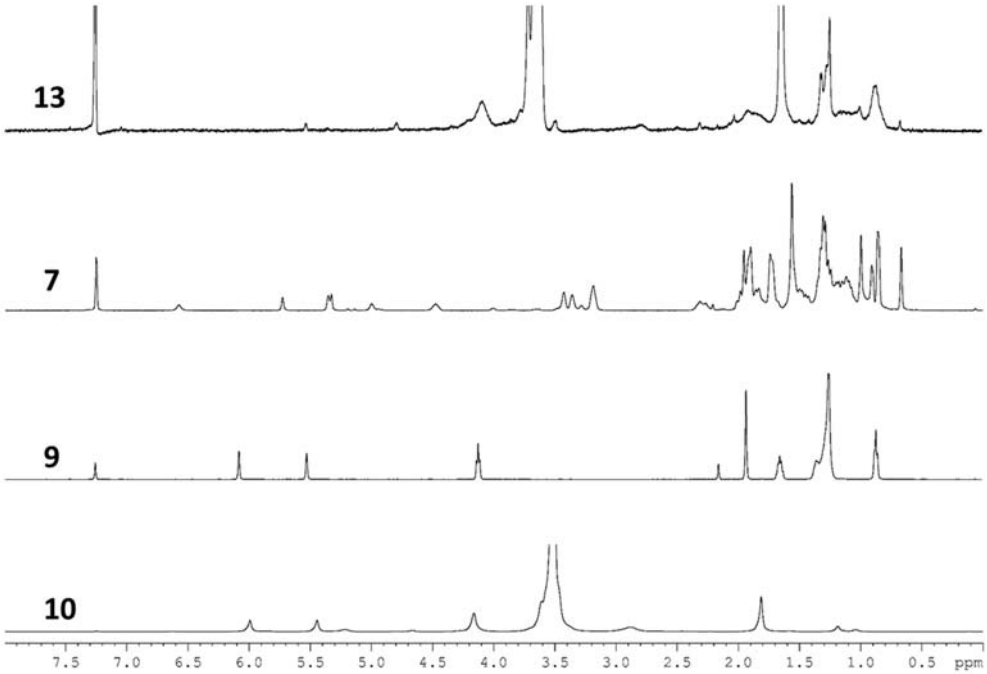

*Figure 4. Stacked NMR of polymer **13** and monomers **7**, **9** and **10**.*

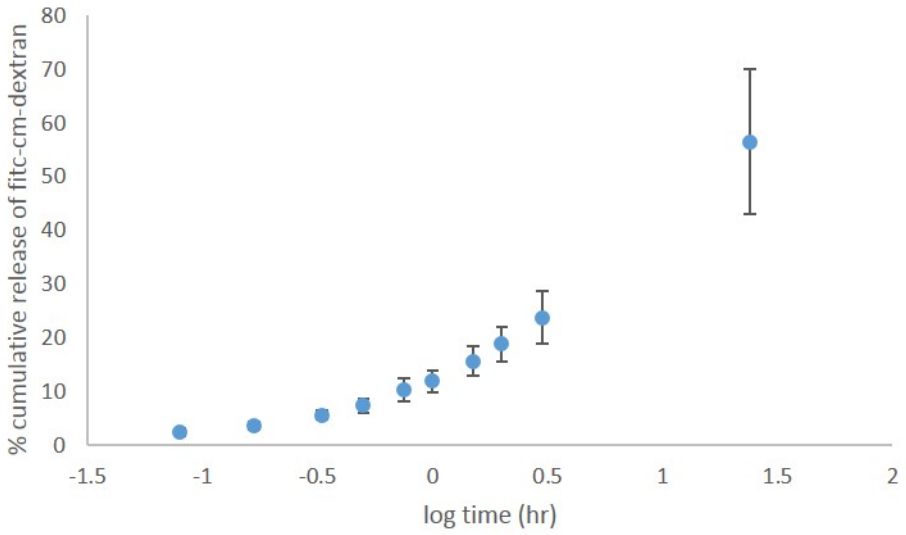

*Figure 5. In-vitro release profile of Fitc-CM-dextran from polymersome prepared from polymer **13** carried out under sink conditions at 37^{0}C.*

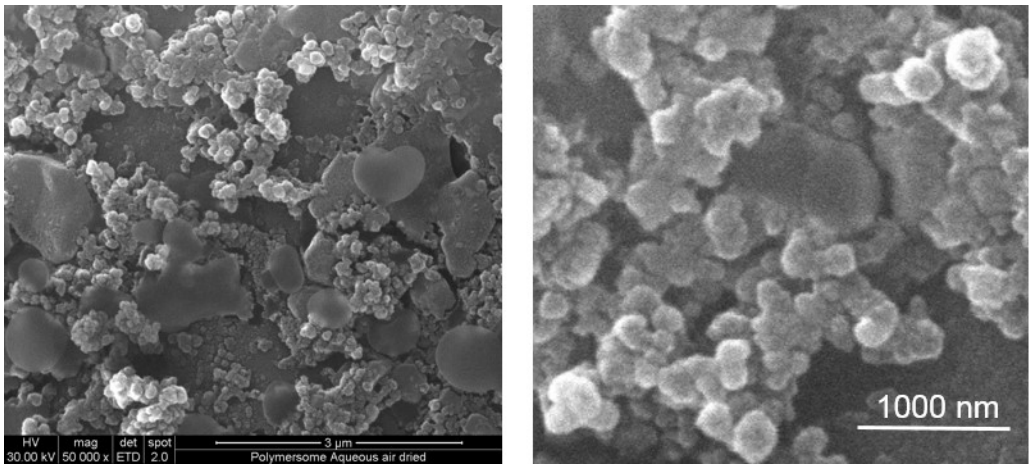

*Figure 6. SEM images of polymersome prepared from polymer **13***

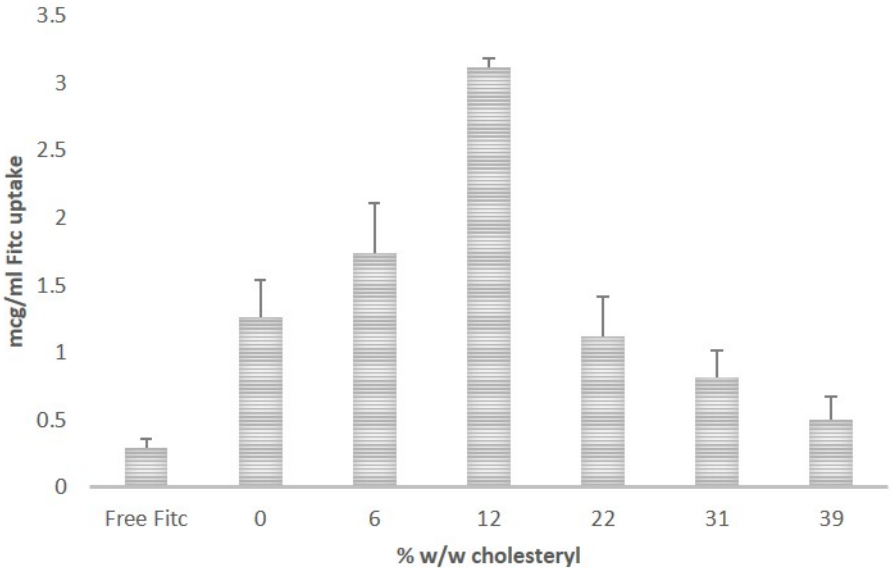

Figure 7. Hela cellular uptake of polyrmersomes encapsulating Fitc-CM dextran with varying amounts of cholesteryl compared with free Fitc-CM-dextran

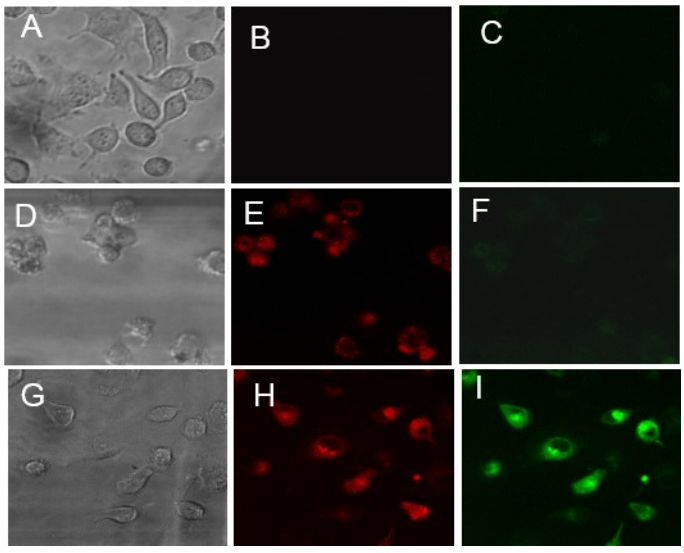

Figure 8. Confocal images of Hela cells incubated with either no drug (A-C), DOX-HCl (D -E) or polymersomal DOX-HCl (G-H). All images have been incubated with CellLight® Reagent BacMam 2.0 GFP as a *late stage endosomal stain. Images A D and G are bright field images. All remaining images are fluorescence emission with an excitation wavelength of 474 and 480 nm, emission collected between 490 and 540 (C,F,I) and 560 – 620 (B, E,H).*

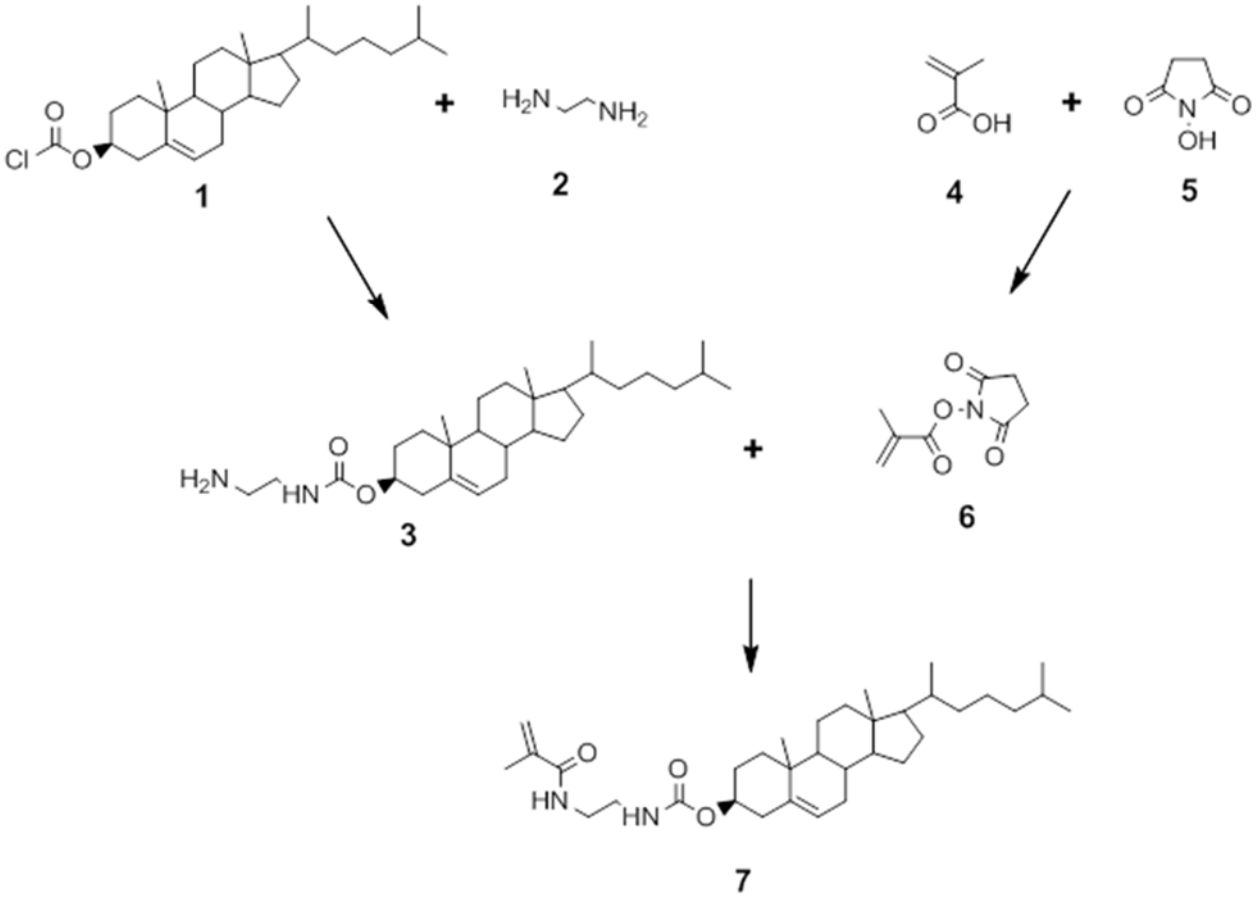

*Scheme 1. Synthesis of monomer **7***

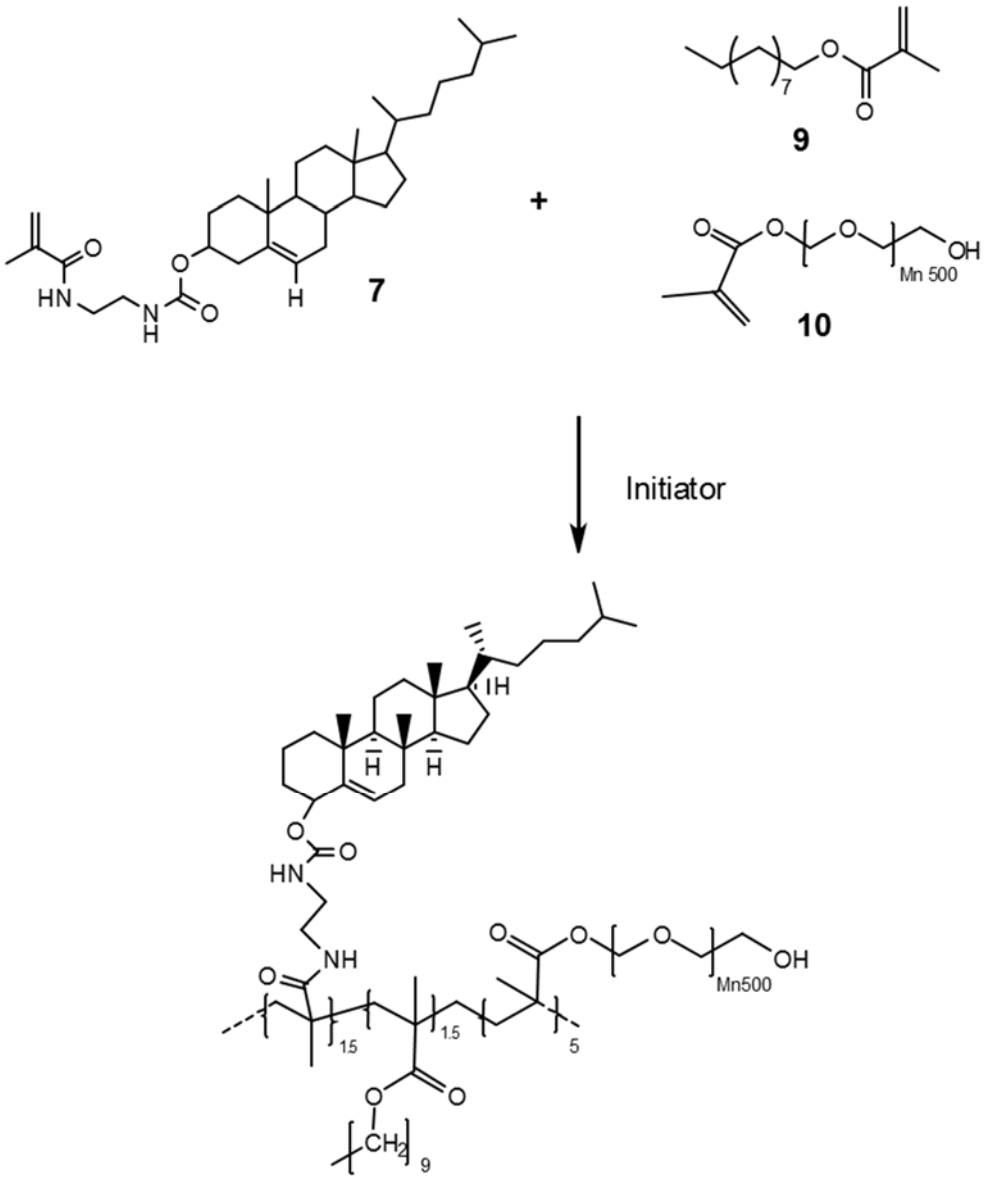

Scheme 2. Synthesis of polymer **14** (for illustration purposes; exact structure may vary).

Table 1. Spectral position and confirmation of specific NMR peaks aligned to Figure 3.

Spectral shift (ppm)	No. of protons	multiplicity	Assigned H	Proton assigned from Figure 3
6.61	1	s	$NHCH_2CH_2NH$	i
5.73 and 5.36	2	d	$C=CH_2$	h
5.29	1	s	$-C=CHCH_2-C$	c
5.01	1	s	$-CH_2CH_2NHCOO-$	j
4.50	1	s	$-(-CH_2-)_2-CHCO_-$	d
3.43-3.29	2	m	$NH_2CH_2CH_2NHCOO-$	e
3.36-3.20	2	m	$NH_2CH_2CH_2NHCOO-$	f
3.19	3	s	$-CH_3C=CH_2$	g
2.32-0.67	39	broad	Steroidal backbone	b
0.67	6	s	$CH_2CH_2CH_2CH(CH_3)_2$	a

Table 2. Different molar ratios of cholesteryl and decyl used to create polymers and subsequent w/w values

Polymer number	Molar ratio*		%w/w		
	cholesteryl	decyl	cholesteryl	decyl	PEG
11	0	0.6	0	21	79
12	0.075	0.525	6	18	76
13	0.15	0.45	12	15	73
14	0.3	0.3	22	9	69
15	0.45	0.15	31	4	64
16	0.6	0	39	0	61

* molar ratio compared to 1Meq PEG

Table 3. Size, PDI and encapsulation efficiency of varying polymers

Polymer number	Size (nm)	PDI	% encapsulation efficiency
11	177 ±6.6	0.53 ± 0.08	52 ± 10
12	103 ± 5.5	0.76 ± 0.13	60 ± 12
13	197 ± 7.4	0.37 ± 0.15	59 ± 3
14	295 ± 60	0.39 ± 0.10	ND
15	299 ± 53	0.53 ± 0.03	ND
16	586 ± 47	0.76 ± 0.13	ND

ND = Not determined n = 3